Eur. Phys. J. Plus (2024) 139:447
https://doi.org/10.1140/epjp/s13360-024-05236-6

THE EUROPEAN PHYSICAL JOURNAL PLUS

Regular Article

# Grazing-sliding bifurcation induced extreme large-intensity pulses in $CO_2$ laser

**S. Leo Kingston**[a]

Division of Dynamics, Lodz University of Technology, Stefanowskiego 1/15, Lodz 90-924, Poland

Received: 18 December 2023 / Accepted: 30 April 2024


**Abstract** We report the formation of extreme large-intensity pulses in an optically modulated CO2 laser. The sudden unexpected surge from the bounded chaotic motion into occasional expansions occurred in the system, which is rare but appears in an infrequent time interval. The CO2 laser exhibits unforeseen extreme pulses owing to the dynamical process of grazing-sliding bifurcation. To acquire a deeper understanding of its intricate dynamics, we have performed various comprehensive dynamical and statistical analyses that elucidate the transition of extreme pulses, and their emerging mechanisms. In addition, we have presented a prior anticipation technique of rare large-intensity pulses that will be shedding into the light for some specific applications.

## 1 Introduction

Recently, a wide range of research has addressed the distinct formation of various catastrophic events, namely rogue waves in hydrodynamics and optical system [1–3], rare but recurrent unexpected large-amplitude events in a different complex systems [4–6], as well as the natural extreme events such as, earth-quicks, cyclones, droughts, and share market crashes [7]. Precisely, in the past few decades, the complex dynamical systems of neuron models [8–11], lasers [12–15], mechanical systems [16, 17], electronic circuits [18, 19], coupled systems [20, 21], and networks of oscillators [22–24] studied in details to ascertain its dynamical origin and different formations. Importantly, the laser models have received significant attention owing to their novel applications. Especially, their utilization is involved in the largest parts of medical treatments, as well as science and engineering appliances. The prime goal of exploring various comprehensive analyses of distinct catastrophic dynamics would have substantial benefits in developing an effective prediction technique and improving mitigation analogies. In recent years, a few natural extreme events have led to a prodigious impact on the environment and human life. As a consequence, an extended rigorous understanding of the distinct formation of extreme events in various complex systems is still a demanding problem to attain the aforementioned intent.

Different emerging mechanisms, as well as transitions of extreme events or rogue waves, have been explored in a diversified class of laser models [12, 13, 25–28]. The innovative work done by Solli *et al*. reported in Ref. [12] explored the emergence of rogue wave in optical experiment which creates a new inroad to identify the substantial possible in the formation of extreme large-intensity pulses in various optical systems. Mercier *et al*., [13] reported the pivotal role of phase-conjugate feedback and time delay effect in the formation of various types of extreme events in a laser diode. In a spatially extended microcavity laser, a specific kind of deterministic spatiotemporal chaotic dynamics induced extreme events illustrated using numerical and experimental studies [25]. The concurrent appearance of rare large-intensity pulses and hyperchaotic dynamics via distinct routes namely, quasiperiodic breakdown to chaos followed by extreme pulses via crisis-induced intermittency dynamics, quasiperiodic intermittency, and Pomeau–Manneville intermittency has been illustrated in a higher dimensional system of Zeeman laser model [26]. Besides, a mid-infrared quantum cascade laser exhibits burst-like extreme events with the influence of external optical feedback and later explored the aspect to set up this model as an all-optical neuromorphic system [27]. The prominent types of intermittencies which lead to the occurrence of large-intensity pules in a higher dimensional laser model and the impact of noise and time delay in their distinct transitions from regular or chaotic dynamics to extreme large pulses are illustrated in details in Ref. [28].

It has reported that different configurations of $CO_2$ lasers were used to demonstrate various complex dynamical behaviors [16, 29–34]. Over three decades before, $CO_2$ laser was used as one of the pioneering experiments to verify desperate nonlinear behavior due to its versatility, as well as the flexibility of their realization [30, 31]. The different classifications of laser spiking, regular, and irregular self-pulsation dynamics studied in $CO_2$ laser using instantaneous or delayed modulation parameters [32]. Stabilization of unstable periodic orbits embedded with discrete strange attractors illustrated using numerical and experimental studies in a loss-driven $CO_2$ laser [33]. Roy *et al*. studied in Ref. [34] synchronization dynamics in a different configurations of $CO_2$ laser. In addition, $CO_2$ laser is involved in widespread usages in the material manufacturing process, medical appliances, and military operations [35,

[a] e-mails: kingston.cnld@gmail.com; leo.sahaya-tharsis@p.lodz.pl (corresponding author)

Published online: 28 May 2024

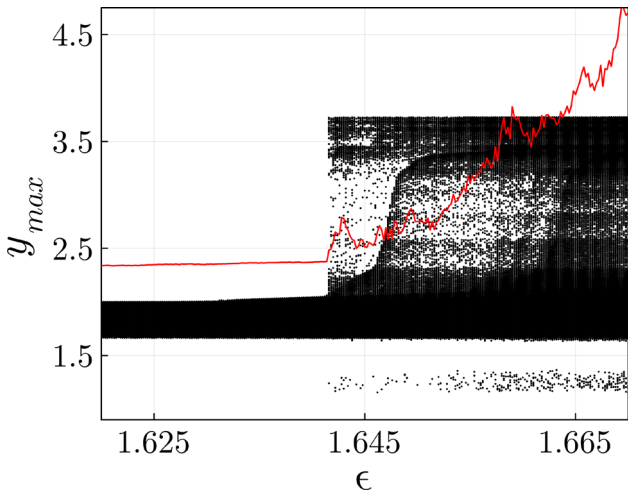


**Fig. 1** One parameter bifurcation diagram of $CO_2$ laser model manifests a sudden surge from bounded chaotic motion into rare large-intensity pulses in $y_{max}$. The red line signifies the extreme events qualifier threshold of $H_s$ to discriminate the existence of extreme pulses and other dynamics in the system

36]. Remarkable, advantages of $CO_2$ laser in medical treatment play a virtual role in different stages. For example, $CO_2$ laser-based equipment acted as a paramount, accurate, and risk-free to proceed discrete dermatology surges [37]. Besides, it is expedient in other medical fields such as neurosurgery, plastic surgery, and otorhinolaryngology discussed in detail Ref. [38]. Certainly, it is of substantial importance to understand the formation of distinct anomalous behavior in the $CO_2$ laser, for the better utilization of the aforementioned applications. Recently, the periodically modulated $CO_2$ laser elucidates the formation of extreme and superextreme events through nonlinear resonance route [29]. Later, an extensive analysis of this $CO_2$ laser revealed that extreme events emanating via stick–slip bifurcation [16] when the trajectories appear closer to the discontinuous region of the system. However, in this present study, we have explored the appearance of extreme pulses through the dynamical process of grazing-sliding bifurcation in a modified version of $CO_2$ laser using various statistical and dynamical analyses.

The remaining part of the paper is presented as follows: the description of optically modulated $CO_2$ laser and its parameter's detail given in Sect. 2. Numerical simulation results of transition to extreme pulses from the bounded chaotic dynamics and their origin are discussed using relevant measures in Sect. 3. The mechanism behind the formation of extreme pulses in the considered model is explored in detail in Sect. 4. The penultimate section elicits the possible prediction of extreme pulses in the $CO_2$ laser. In the final section, we have explained the overall summary of our results.

## 2 $CO_2$ laser model

We have considered an optically modulated $CO_2$ laser model [34, 39], in order to demonstrate the various intricate dynamics in the system including extreme large-intensity pulses. The governing equations of the model in the normalized form are given as follows:

$$\begin{aligned}\dot{x} &= x[l_1(y - 1.0 - k_1 \sin^2 z) - l_3\epsilon \cos(l_2 t)] \\ \dot{y} &= -(y - n) - 2l_1 xy \\ \dot{z} &= -l_4\left(z - b + \frac{rx}{1 + \zeta x}\right).\end{aligned} \tag{1}$$

Here, $l_1 = k_0/\gamma, l_2 = \Omega/\gamma, l_3 = k/\gamma, l_4 = \beta/\gamma, n = \frac{\alpha N_0}{k_0}, r = \frac{\pi k_0 R}{\alpha V_\lambda}$, and $\zeta = \frac{\eta k_0}{\alpha}$ are the normalized system parameters. Here, $k_0$ and $k$ denote cavity length and total transmission time in the model system. Besides, $N_0$, $\beta$, $\Omega$, $\eta$ $\gamma$, $R$, and $V_\lambda$ signify the pumping power, damping rate, frequency of the driving modulation, nonlinearity of detection apparatus, total gain feedback, and half-wave voltage. The parameter $\alpha$ represents the coupling coefficient value which is used for both laser intensity and population inversion of the system; more details of the model are given in Refs. [34, 39]. For different values of $r$, modulation depth $\epsilon$, and bias voltage $b$, we have identified distinct complex dynamics in the $CO_2$ laser.

We have solved the system Eq. (1) using $4^{th}$ order Runge–Kutta method using the step size of 0.001. Throughout this paper, unless otherwise mentioned, we have fixed the system parameters value of $l_1 = 28.57, l_2 = 30.0, l_3 = 25.0, l_4 = 6.452, n = 4.0, b = 4.5$, and $\zeta = 25.57$ based on the Ref. [34]. Further, for a fixed $r = 200$ and gradually increasing the modulation depth value $\epsilon$ in a specific range, the $CO_2$ laser exhibits different convolution dynamics. More details on the formation of extreme events, as well as their transition, will be explored in the upcoming sections.

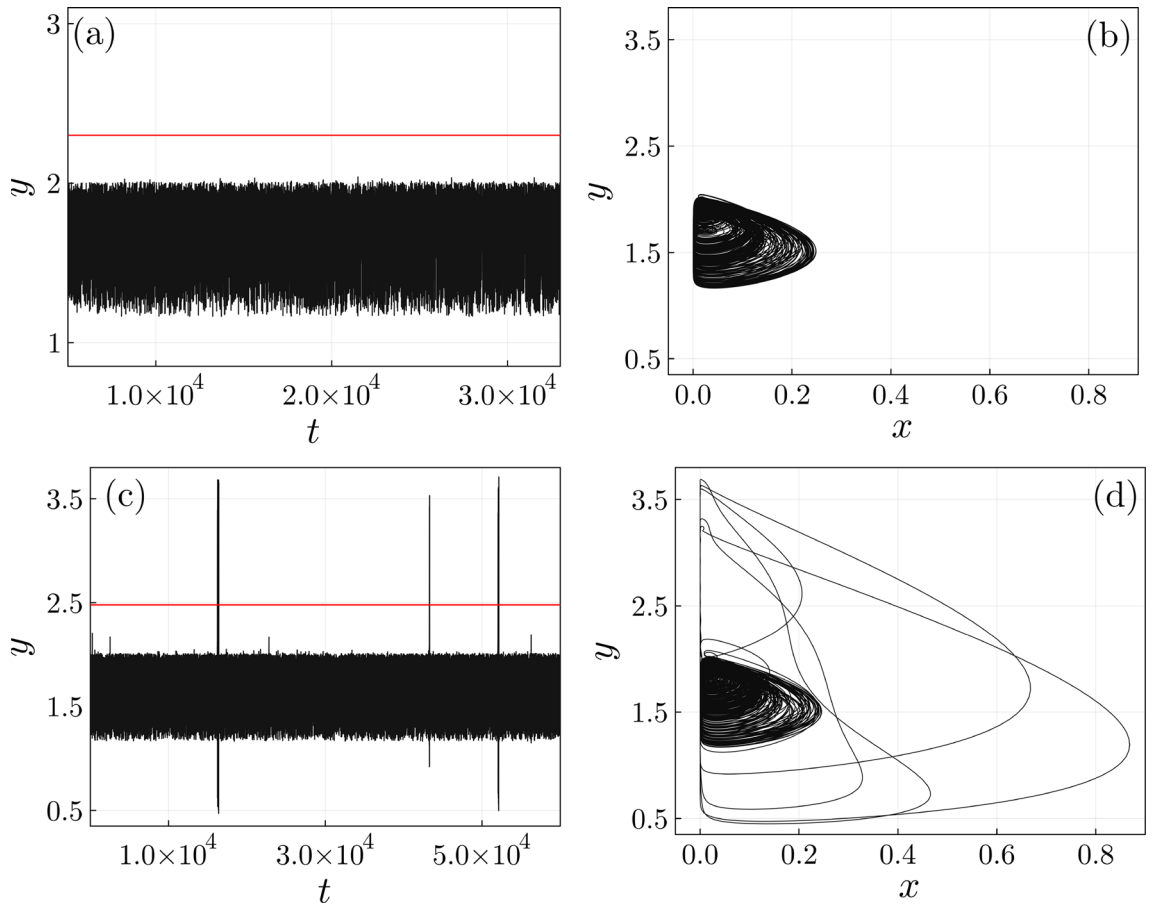


**Fig. 2** Temporal dynamics and phase portraits of $CO_2$ laser: (**a**) and (**b**) bounded chaotic dynamics, (**c**) and (d) extreme pulses appear from the bounded motion in irregular time intervals. Horizontal red lines in the time series of (**a**) and (**c**) denote the significant height threshold $H_s$

## 3 Extreme pulses in $CO_2$ laser model

In this section, we elaborate on the formation of unforeseen extreme pulses in the $CO_2$ laser. First, we have presented a one parameter bifurcation diagram for the fixed system parameters as mentioned in the previous section and for fine-tuning of $\epsilon \in (1.62, 1.67)$ in Fig. 1. The system oscillates within a bounded chaotic state for the control parameter values $\epsilon < 1.6415$. When we slightly increase $\epsilon > 1.6415$, the $CO_2$ laser manifests occasional extreme pulses from the bounded region. To ascertain the appearance of extreme events in the system, we have calculated a significant height threshold $H_s$, which is plotted as a red line in the bifurcation diagram of Fig. 1. The qualifier threshold is defined as $H_s = \langle y_n \rangle + n\sigma$, where $y_n = y_{max}$ is the local maxima of time series and $\sigma$ denotes its corroborate standard deviation. Here, we have taken the value of $n = 6$ for our analysis. It can be obtained from Fig. 1, for a range of chaotic state $\epsilon \in (1.62, 1.6415)$, the qualifier threshold placed over the chaotic attractors. Conversely, for the range modulation depth values $\epsilon \in (1.6416, 1.6645)$, the extreme pulses cross the significant height threshold. Once again, the $H_s$ values are located above for the large expanded attractors as well, since for the parameter values $\epsilon > 1.6645$, the $CO_2$ laser reveals more frequent large expansions. According to the fundamental definition, the multiple existences of large-intensity pulses cannot be classified as extreme events.

Further, to elucidate more details on the formation of large-intensity pulses from the bounded chaotic states, we have plotted distinct time series and phase portraits as shown in Fig. 2a–d. The time series of $y(t)$ manifests chaotic dynamics for $\epsilon = 1.6415$ depicted in Fig. 2a; here, the system oscillates within a specific range of the bounded region. Its equivalent phase portrait is shown in Fig. 2b. On the other hand, for a further slight increase of $\epsilon = 1.6416$, the $CO_2$ laser proves occasional extreme pulses from the bounded chaotic motion in an irregular time durations that represented in Fig. 2c. The time series plots of Fig. 2a and c clearly denoted that the qualifier threshold placed above for chaotic states, whereas the extreme pulses cross the significant height threshold $H_s$. The phase portrait of extreme large-intensity events is proved in Fig. 2d. Remarkably, when the trajectories approach very close to the discontinuous boundary at zero, a specific kind of sliding motion appears in the system. As a result, abrupt extreme pulses appeared in the system. More details on how these unexpected large deviations occur and the relevant mechanism behind them will be explained in the following section.

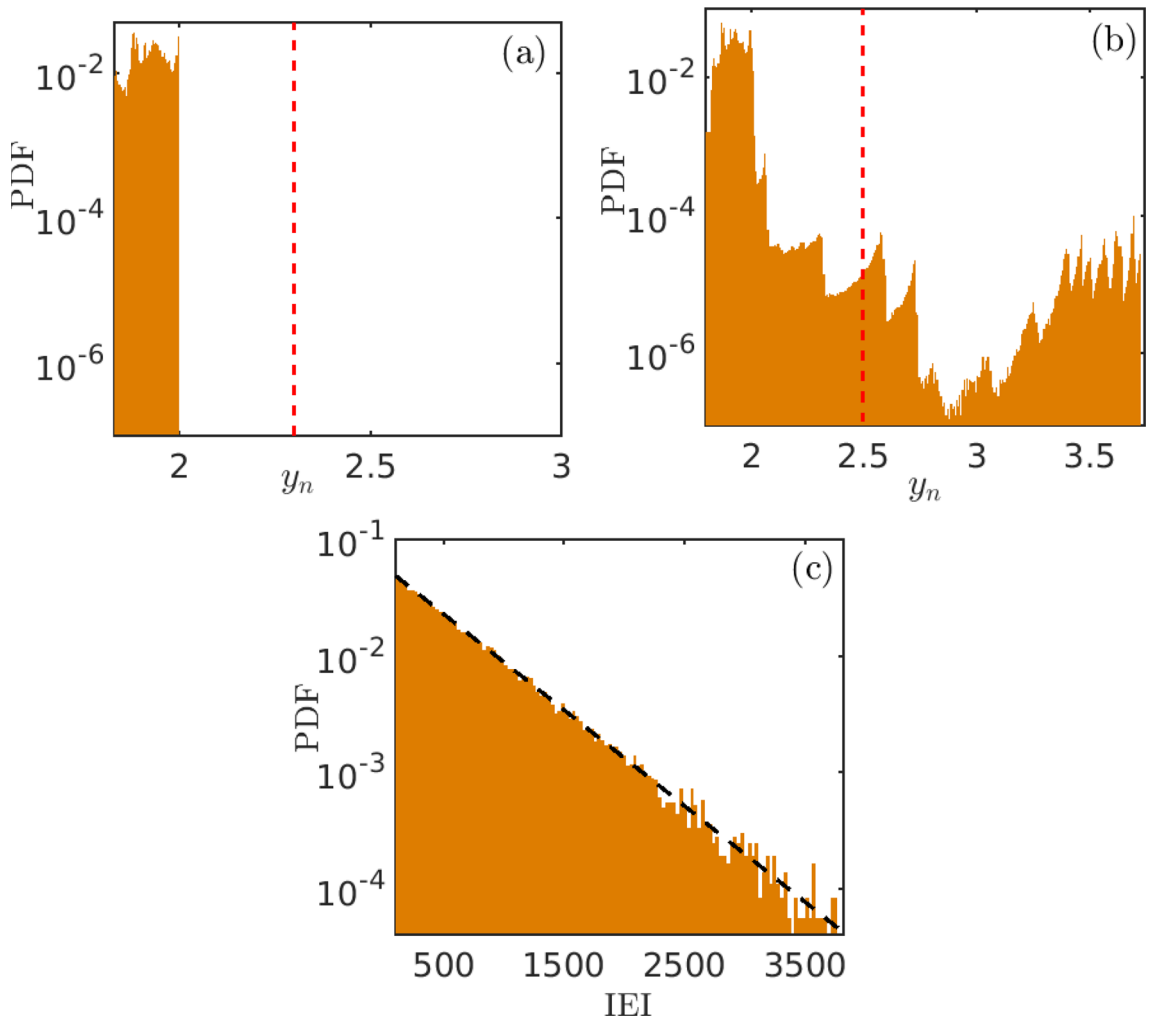


**Fig. 3** Probability distribution functions: (**a**) chaotic state at $\epsilon = 1.6415$, the distribution confined in a bounded range, and the $H_s$ line placed away from the bounded region. (**b**) Lower probability of occurrence of extreme pulses in the tail region which crosses the significant height threshold for $\epsilon = 1.6416$. In both (**a**) and (**b**), the vertical-dashed lines signify the extreme events' qualifier threshold. (**c**) Inter-event intervals distribution of extreme events time series for $\epsilon = 1.6416$ proves a Poison-like distribution and fitted by an exponential function (black-dashed line)

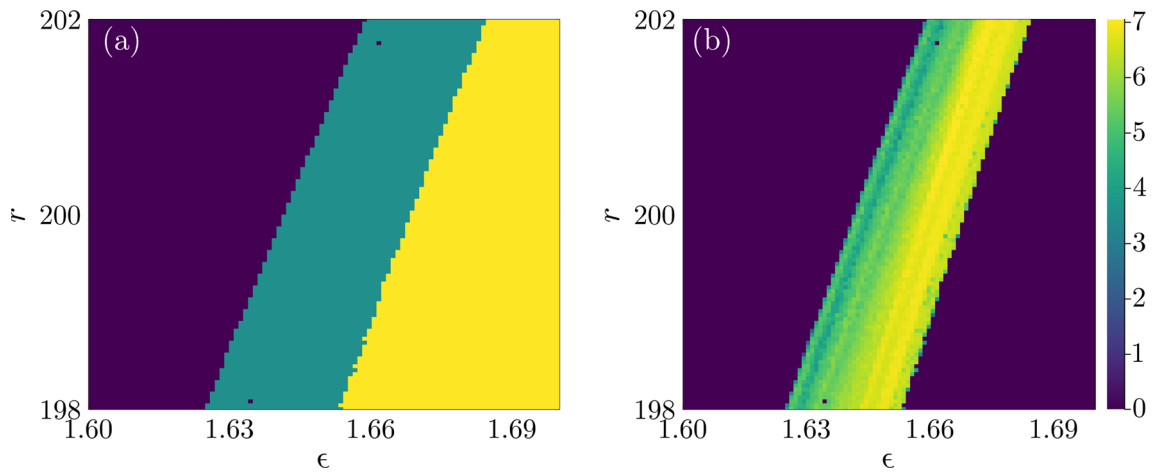


**Fig. 4** **a** The two-parameter phase diagram in the $\epsilon$ versus $r$ plane manifests the existence of bounded chaos (dark magenta), extreme pulses (dark cyan), and multiple large-intensity pulses (yellow) in a wider parameter range. The counts of rare and large-intensity pulses that exceeded the significant height threshold in (**b**) manifest the variation of extreme pulses in a range of system parameters. The color bar in (**b**) is presented as a log scale for better visualization

We have drawn the probability distribution function (PDF) for both chaotic and extreme events' time series to demonstrate the different aspects of the discrete complex dynamics in the $CO_2$ laser model. For calculating PDFs, we have taken a significantly larger length of time series data after discarding sufficient transient time. Figure 3a portrays the PDF for chaotic dynamics for $\epsilon = 1.6415$ representing the existence of chaotic states in a restricted region and also located below the significant height threshold (vertical dashed line). Conversely, for a larger value of modulation depth $\epsilon = 1.6416$, we have obtained a completely different shapes of the distribution. Indeed, the occasional extreme pulses manifest a lower probability of their occurrence as compared with the predominant probability of appearance in the bounded chaotic states, which is pictured in Fig. 3b. Hence, the PDF plot of Fig. 3b depicts a heavy-tail distribution, which is a peculiar characteristic behavior of extreme events. In addition, we have confirmed that the shape of the PDF of Fig. 3b is robust with respect to the different lengths of data taken for our analysis. Besides, in the tail region, the rare large-intensity pulses exceed the qualifier threshold ($H_s$). The $H_S$ values for chaotic and extreme pulses are calculated from their respective time series data.

Moreover, it is worthwhile to investigate the relation of the time difference between the consecutive extreme pules for a larger range of temporal data. To perform such analysis, we have calculated the inter-event intervals (IEIs) of successive extreme pulses and its corroborate PDF is showcased in Fig. 3c. The IEI probability distribution function for $\epsilon = 1.6416$ reveals a Poison-like distribution denotes that the uncorrelated nature of the return time of successive extreme large-intensity pulses in the system. Further, we have fitted the IEI probability distribution function with exponential decay function $P(\text{IEI}) = ae^{(-b\text{IEI})}$ as a dashed line in Fig. 3c. The fitting parameters value is chosen as $a = 0.0588$ and $b = 0.0018$.

Furthermore, we have illustrated that the formation of extreme large-intensity pulses in $CO_2$ laser is not restricted to a specific range of control parameter value of modulation depth $\epsilon$ and a fixed $r = 200$. We have identified the appearance of extreme pulses in a specific range of parameter space while analyzing a distinct range of parameter values. Accordingly, a two-parameter phase diagram portrayed in Fig. 4a, for a wide range of $\epsilon \in (1.60, 1.70)$ and $r \in (198.0, 202.0)$. In order to discriminate the existence of bounded chaotic (dark magenta), extreme pulses (dark cyan), and multiple large-intensity pulses (yellow), we have used the significant height threshold measure. The $CO_2$ laser model proves the advent of extreme large-intensity pulses for a specific range of parameter regions (a dark cyan region in Fig. 4a). For a rigors analysis, near the transition point of Fig. 1, the system manifests only a few rare extreme pulses. Nevertheless, a gradual increase of modulation depth $\epsilon$ reveals a moderate increase in the number of extreme pulses in $CO_2$ laser. Later, the system exhibits more frequent large expanded pulses for the higher values of modulation depth (when parameter values reside in the yellow region of Fig. 4a) denoting that there is no significance in the existence of extreme pulses. Hence, it is worth investigating the variation in the number of extreme pulses for a specific range of system parameter space. For that, we define the quantity *counts* which represent the sum of a number of extreme pulses that exceed the significant height threshold; the mathematical definition of this measure is discussed in detail [28]. The resultant count plot for a broader range of parameter space is portrayed in Fig. 4b. The number of extreme pulses (counts) is represented as a color bar with a log scale for a preview of better visualization. It can be inferred from Fig. 4b that the number of extreme events is gradually increasing and it attains a significant quantity in the specific parameter range (color ranges of dark cyan to light yellow). Further, varying the modulation depth values, the number of extreme pulses decreases sharply and finally turns into a large expanded chaotic region (dark magenta).

## 4 Mechanism: extreme pulse formation

In this section, we have illustrated the mechanism that is responsible for the formation of extreme pulses in the $CO_2$ laser. For that, the vector field of the system is drawn for a specific range of system variables depicted in Fig. 5(a). Intriguingly, the system manifests a discontinuous boundary $\Sigma_s$ at $x = 0.0$, which is highlighted by blue and light yellow colors, respectively. These discontinuous regions discriminate two different subspaces $S_1$ and $S_2$, that is, $x > 0.0$ is one side $S_1$, and $x < 0.0$ is another side $S_2$. The vector field aligns parallel with the discontinuous boundary. Within the shaded blue region, the vector field along the discontinuous boundary directs the trajectory outward. This outward direction continues until reaching $y = 4$. At $y = 4$, the trajectory's direction changes downward, marked by the dashed red line. This alteration in the vector field's direction at the discontinuous boundary (light yellow region) defines the maximum amplitude of laser pulses, a topic to be discussed shortly. Exploring how the extreme large-intensity pulses manifest in the laser system, the choice of an initial condition $x_0$ in the $S_1$ region results in diverse attractors depending on the trajectory's distance from the discontinuous boundary. Close proximity to the boundary leads to different types of periodic or chaotic attractors. Notably, trajectories approaching very close to the discontinuous region, a phenomenon known as grazing dynamics, and exhibiting proximity to the discontinuous boundary experience sliding dynamics.

In sliding dynamics, the trajectory is trapped near the discontinuous boundary and slides along it following the vector field direction, causing significant expansion due to the dynamical behavior of grazing-sliding bifurcation. Sliding occurs maximally up to $y = 4$, coinciding with the change in the vector field's direction. This change rejects the trajectory from the discontinuous boundary, leading it to be repelled toward the subspace $S_1$. The maximum values of the large excursion intensity are also supported by the probability distribution plot of Fig. 3b, where the uttermost intensity of the system for extensive temporal evolutions is located less than four. Note that, long excursions occur when the trajectory is trapped and sliding along the discontinuous boundary. It is crucial to note that during grazing, trajectories do not approach the $S_2$ subspace, as the lasers' intensity cannot take on negative values.

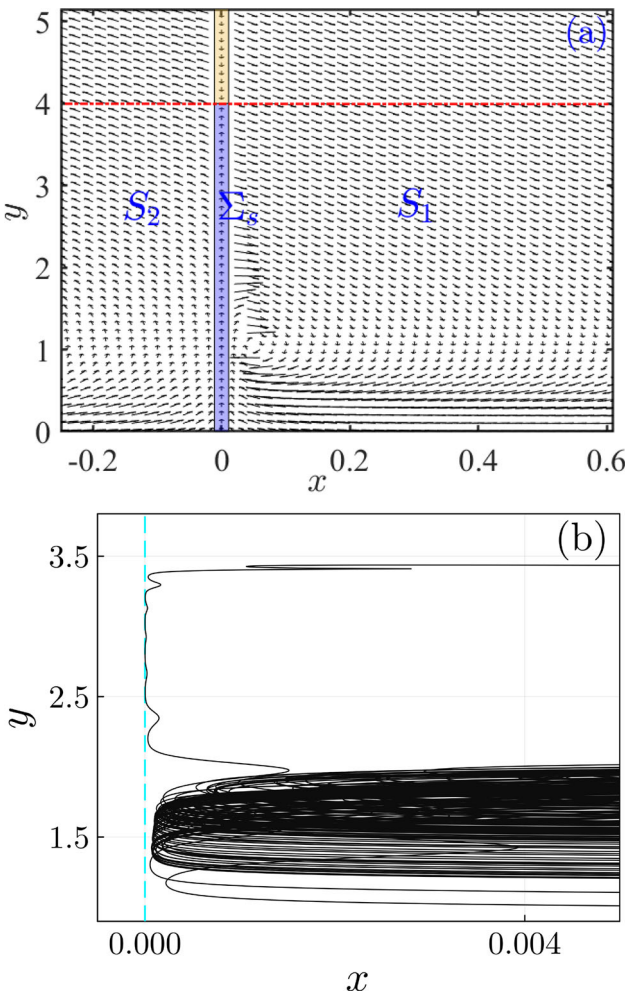


**Fig. 5** (**a**) Vector field plot of $CO_2$ laser manifests the existence of two subspace $S_1$ and $S_2$ that is separated by a discontinuous boundary $\Sigma_s$. (**b**) A magnified phase of extreme large-intensity pulses and a vertical dashed line (cyan) signifies the discontinuous boundary of the system

To ascertain more clarity of these dynamics, we have plotted a magnified phase portrait that exhibits extreme pules as shown in Fig. 5b. The discontinuous region plotted as a dashed cyan line at $x$ is equal to zero. It is clear from Fig. 5b that during the bounded chaotic motion, the trajectories do not approach the discontinuous boundary. However, for a particular time interval, the trajectory undergoes grazing as well as sliding dynamics which create a very large excursion from the bounded region of the system. Notable, Suresh *et al*. reported in Ref. [16] that stick–slip dynamics induced extreme events in MEMS and parametrically driven $CO_2$ laser model. In that case, large expansion originated only because of stick–slip bifurcation. Indeed, the stick–slip bifurcation is a generous concept that illustrates an alternate appearance of sticking and slipping motion in the system. On the other hand, grazing-sliding bifurcation takes place in a system owing to the near conduct dynamics of a trajectory with a sliding surface which creates a sudden catastrophic shift in the system dynamics.

## 5 Prediction of extreme pulses in $CO_2$ laser

Finally, we have shown a simple and effective dynamical system approach to earlier prediction for extreme pulses in $CO_2$ laser. To explore that, the magnified times series of both $x(t)$ and $y(t)$ is presented in Fig. 6a and b. First, we illustrate the reason behind the existence of two distinct extreme pulses ($ep_1$ and $ep_2$) with different amplitude in the system. Indeed, the appearance of different amplitudes of extreme pulses depends on how closely the trajectories undergo into the discontinuous boundary. For example, the extreme pulses $ep_2$ approach double times close to the discontinuous boundary as compared with $ep_1$, consequently, it manifests a much larger expansion which is clearly shown in Fig. 6. In addition, there exists an intriguing relation between the commence timing of sliding ($t_{sl}$) and the timing of the emergence of extreme pulses crossing the threshold ($t_{ep}$) in the system presented in Fig. 6b. Note that, the extreme pulses are not exhibited in the system at all times of the sliding process. For instance, if the trajectory undergoes a shorter sliding motion and does not cross the qualifier threshold value (dashed red line), then the $CO_2$ laser does not exemplify extreme pulses. Conversely, when the trajectory experienced a longer sliding motion near the discontinuous region, it led to the emergence of extreme pulses in the system that also exceeded the significant height threshold value. For more clarity in this

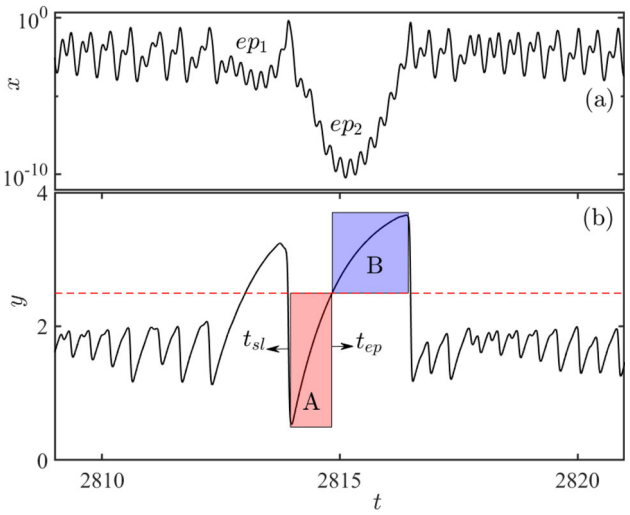


**Fig. 6** Extreme pulse forecasting in $CO_2$ laser. Magnified time series of $x(t)$ (**a**) and $y(t)$ (**b**) manifest two consecutive extreme pulses ($ep_1$ and $ep_2$). Shaded red (A) and blue (B) regions in (b) signify distinct sliding regions of the system

illustration, the sliding region of the trajectories splits into two parts: A and B. It is inferred Fig. 6b that if the trajectories sustained within region A (shaded red region) prove the existence of non-extreme pulses in the system. On the other hand, when the trajectories reach region B (shaded blue region), we can obtain the extreme pulses in the system. The time duration of A+B is the total sliding time. While the B can be considered as the duration of extreme events. If the duration is less than or equal to A, then the events become normal events. Along with one can determine, how close the trajectories are to the discontinuous boundary in a $x$ variable, which is used to identify the sliding distance of the trajectories in the $y$ variable. Moreover, the time difference between $t_{ep}$ - $t_{sl}$ is known as early prediction time before the system emanates extreme pules. Noteworthy, an earlier prediction of extreme events in various engineering models can be more beneficial to initiate early warnings, before the occurrence of catastrophic consequences that are based on the specific system requirements.

## 6 Conclusion

In summary, we have identified the formation of extreme large-intensity pulses in the optically modulated $CO_2$ laser model. The system manifests discrete complex dynamics for different choices of the system parameters. An abrupt surge appeared in the model from the bounded motion into occasional large-intensity pulses. The extreme pulses emanated owing to the grazing-sliding dynamics when the trajectories approached proximity to the discontinuous boundary of the system. We have presented discrete statistical measures, namely significant height threshold, probability distribution function, and inter-event interval distribution to ascertain the rare occurrence of extreme pulses in the system. In addition, we have shown the advent of extreme large-intensity pules in a parameter space using the phase diagram. Besides, the distribution of a number of large-intensity pulses is shown as the counts plot in a specific region of parameters in the system. Finally, we have illustrated the feasible early prediction of rare large-intensity pulses in a $CO_2$ laser. Overall, these observations will provide better insight into the formation of specific unforeseen dynamics in the laser model and the necessity of the awareness of their appearance while utilizing in the discrete application. Also, the proposed forecasting analysis would be helpful to enhance the mitigation techniques.

**Acknowledgements** This work is supported by the National Science Centre, Poland, OPUS Programs (Projects No. 2018/29/B/ST8/00457, and 2021/43/B/ST8/00641). The author likes to thank Suresh Kumarasamy and Tomasz Kapitaniak for the interesting discussion.

**Data Availability Statement** Datasets generated during the current study are available from the corresponding author on reasonable request. The manuscript has associated data in a data repository.

## References

1. M. Onorato, S. Residori, U. Bortolozzo, A. Montina, F. Arecchi, Rogue waves and their generating mechanisms in different physical contexts. Phys. Rep. **528**(2), 47–89 (2013)
2. K. Dysthe, H.E. Krogstad, P. Müller, Oceanic rogue waves. Annu. Rev. Fluid Mech. **40**, 287–310 (2008)
3. N. Akhmediev, B. Kibler, F. Baronio, M. Belić, W.-P. Zhong, Y. Zhang, W. Chang, J.M. Soto-Crespo, P. Vouzas, P. Grelu et al., Roadmap on optical rogue waves and extreme events. J. Opt. **18**(6), 063001 (2016)
4. M. Farazmand, T.P. Sapsis, Extreme events: mechanisms and prediction. Appl. Mech. Rev. **71**(5), 050801 (2019)
5. A. Mishra, S.L. Kingston, C. Hens, T. Kapitaniak, U. Feudel, S.K. Dana, Routes to extreme events in dynamical systems: dynamical and statistical characteristics. Chaos Interdisc. J. Nonlinear Sci. **30**(6), 063114 (2020)

6. S.N. Chowdhury, A. Ray, S.K. Dana, D. Ghosh, Extreme events in dynamical systems and random walkers: A review. Phys. Rep. **966**, 1–52 (2022)
7. S. Albeverio, V. Jentsch, H. Kantz, *Extreme Events in Nature and Society* (Springer, Berlin, 2002)
8. G. Ansmann, R. Karnatak, K. Lehnertz, U. Feudel, Extreme events in excitable systems and mechanisms of their generation. Phys. Rev. E **88**(5), 052911 (2013)
9. V. Varshney, S. Kumarasamy, A. Mishra, B. Biswal, A. Prasad, Traveling of extreme events in network of counter-rotating nonlinear oscillators. Chaos Interdisc. J. Nonlinear Sci. **31**(9), 093136 (2021)
10. A. Mishra, S. Saha, M. Vigneshwaran, P. Pal, T. Kapitaniak, S.K. Dana, Dragon-king-like extreme events in coupled bursting neurons. Phys. Rev. E **97**(6), 062311 (2018)
11. S.L. Kingston, T. Kapitaniak, Intermittent large amplitude bursting in Hindmarsh-Rose neuron model. In: 2021 5th Scientific School Dynamics of Complex Networks and Their Applications (DCNA) (2021). IEEE
12. D.R. Solli, C. Ropers, P. Koonath, B. Jalali, Optical rogue waves. Nature **450**(7172), 1054–1057 (2007)
13. É. Mercier, A. Even, E. Mirisola, D. Wolfersberger, M. Sciamanna, Numerical study of extreme events in a laser diode with phase-conjugate optical feedback. Phys. Rev. E **91**(4), 042914 (2015)
14. S. Coulibaly, M. Clerc, F. Selmi, S. Barbay, Extreme events following bifurcation to spatiotemporal chaos in a spatially extended microcavity laser. Phys. Rev. A **95**(2), 023816 (2017)
15. S.L. Kingston, A. Mishra, M. Balcerzak, T. Kapitaniak, S.K. Dana, Instabilities in quasiperiodic motion lead to intermittent large-intensity events in Zeeman laser. Phys. Rev. E **104**(3), 034215 (2021)
16. S. Kumarasamy, A.N. Pisarchik, Extreme events in systems with discontinuous boundaries. Phys. Rev. E **98**(3), 032203 (2018)
17. B. Kaviya, R. Suresh, V. Chandrasekar, Extreme bursting events via pulse-shaped explosion in mixed Rayleigh-Liénard nonlinear oscillator. The Eur. Phys. J. Plus **137**(7), 844 (2022)
18. S.L. Kingston, K. Thamilmaran, P. Pal, U. Feudel, S.K. Dana, Extreme events in the forced Liénard system. Phys. Rev. E **96**(5), 052204 (2017)
19. H.L.D.S. Cavalcante, M. Oriá, D. Sornette, E. Ott, D.J. Gauthier, Predictability and suppression of extreme events in a chaotic system. Phys. Rev. Lett. **111**(19), 198701 (2013)
20. S. Kumarasamy, S. Srinivasan, P.B. Gogoi, A. Prasad, Emergence of extreme events in coupled systems with time-dependent interactions. Commun. Nonlinear Sci. Numer. Simul. **107**, 106170 (2022)
21. S.L. Kingston, T. Kapitaniak, S.K. Dana, Transition to hyperchaos: sudden expansion of attractor and intermittent large-amplitude events in dynamical systems. Chaos Interdisc. J. Nonlinear Sci. **32**(8), 081106 (2022)
22. A. Ray, A. Mishra, D. Ghosh, T. Kapitaniak, S.K. Dana, C. Hens, Extreme events in a network of heterogeneous Josephson junctions. Phys. Rev. E **101**(3), 032209 (2020)
23. A. Ray, T. Bröhl, A. Mishra, S. Ghosh, D. Ghosh, T. Kapitaniak, S.K. Dana, C. Hens, Extreme events in a complex network: interplay between degree distribution and repulsive interaction. Chaos Interdisc. J. Nonlinear Sci. **32**(12), 121103 (2022)
24. S.L. Kingston, G. Kumaran, A. Ghosh, S. Kumarasamy, T. Kapitaniak, Impact of time varying interaction: Formation and annihilation of extreme events in dynamical systems. Chaos Interdisc. J. Nonlinear Sci. **33**(12), 123134 (2023)
25. F. Selmi, S. Coulibaly, Z. Loghmari, I. Sagnes, G. Beaudoin, M.G. Clerc, S. Barbay, Spatiotemporal chaos induces extreme events in an extended microcavity laser. Phys. Rev. Lett. **116**(1), 013901 (2016)
26. S.L. Kingston, M. Balcerzak, S.K. Dana, T. Kapitaniak, Transition to hyperchaos and rare large-intensity pulses in Zeeman laser. Chaos Interdisc. J. Nonlinear Sci. **33**(2), 023128 (2023)
27. O. Spitz, J. Wu, A. Herdt, G. Maisons, M. Carras, W. Elsäßer, C.-W. Wong, F. Grillot, Extreme events in quantum cascade lasers. Adv. Photon. **2**(6), 066001 (2020)
28. S.L. Kingston, S. Kumarasamy, M. Balcerzak, T. Kapitaniak, Different routes to large-intensity pulses in Zeeman laser model. Opt. Express **31**(14), 22817–22836 (2023)
29. C. Bonatto, A. Endler, Extreme and superextreme events in a loss-modulated $CO_2$ laser: nonlinear resonance route and precursors. Phys. Rev. E **96**(1), 012216 (2017)
30. F.T. Arecchi, R. Meucci, G. Puccioni, J. Tredicce, Experimental evidence of subharmonic bifurcations, multistability, and turbulence in a $q$-switched gas laser. Phys. Rev. Lett. **49**, 1217–1220 (1982)
31. C. Bonatto, J.C. Garreau, J.A. Gallas, Self-similarities in the frequency-amplitude space of a loss-modulated $CO_2$ laser. Phys. Rev. Lett. **95**(14), 143905 (2005)
32. J.A.C. Gallas, Spiking systematics in some $CO_2$ laser models. In: Advances in Atomic, Molecular, and Optical Physics, vol. 65. New York, pp. 127–191 (2016)
33. A. Pisarchik, B. Kuntsevich, R. Corbalán, Stabilizing unstable orbits by slow modulation of a control parameter in a dissipative dynamic system. Phys. Rev. E **57**(4), 4046 (1998)
34. A. Roy, A. Misra, S. Banerjee, Synchronization in networks of coupled hyperchaotic $CO_2$ lasers. Phys. Scr. **95**(4), 045225 (2020)
35. W. Duley, $CO_2$ lasers effects and applications, New York (2012)
36. W.J. Witteman, The $CO_2$ Laser vol. 53. Berlin, Germany (2013)
37. T. Omi, K. Numano, The role of the $CO_2$ laser and fractional $CO_2$ laser in dermatology. Laser Ther. **23**(1), 49–60 (2014)
38. M.-H. Lai, K.-S. Lim, D.S. Gunawardena, Y.-S. Lee, H. Ahmad, $CO_2$ laser applications in optical fiber components fabrication and treatment: a review. IEEE Sens. J. **17**(10), 2961–2974 (2017)
39. R. Meucci, A. Labate, M. Ciofini, Controlling chaos by negative feedback of subharmonic components. Phys. Rev. E **56**(3), 2829 (1997)